Arab J Sci Eng (2018) 43:1911–1924
https://doi.org/10.1007/s13369-017-2814-6

RESEARCH ARTICLE - CIVIL ENGINEERING

Dynamic Responses of Sliding Isolation Concrete Rectangular Liquid Storage Structure with Limiting Devices Under Bidirectional Earthquake Actions

Wei Jing[1,2] · **Xuansheng Cheng**[1,2] · **Wei Shi**[3]

Received: 4 May 2017 / Accepted: 20 August 2017 / Published online: 16 September 2017

Abstract There is no lack of destructions of concrete liquid storage structures in the previous earthquake, and concrete rectangular liquid storage structures (RLSSs) are widely used in all kinds of engineering fields, so it is significant to study energy dissipation method aiming at structural responses and wave height. An energy dissipation method combination of sliding isolation and limiting-device is proposed for concrete RLSS, considering fluid– structure interaction, simplified and numerical models of a concrete RLSS with displacement-limiting devices are established. The dynamic responses of sliding isolation concrete RLSS with limiting devices under bidirectional earthquake actions are studied, parameter analysis is conducted, and seismic decrease coefficient is used to evaluate the reduction effect of sliding isolation on concrete RLSS. The results show that damping effect of sliding isolation with limiting devices on concrete RLSS is significant, and the dynamic responses under horizontal bidirectional earthquake actions are obviously higher than that of unidirectional earthquake action. The smaller the friction coefficient is, wall tensile stress and wave height are more reduced; in the premise of keeping the structural displacement within the limit, the limiting-device diameter should be smaller; liquid height mainly affects wall tensile stress and structural displacement. When the friction coefficient and limiting-device diameter are designed reasonably, seismic decrease coefficients corresponding to wall tensile stress and wave height are all large enough. Therefore, the proposed energy dissipation method is of great significance for the prevention and control of the common two types of failure modes (wall cracking and liquid overflow) of concrete RLSSs.

Keywords Liquid storage structure · Sliding isolation · Limiting devices · Shock absorption · FSI · Bidirectional earthquake

1 Introduction

Concrete rectangular liquid storage structures (RLSSs) are widely used in water supply and drainage systems, industrial and agricultural production facilities; however, earthquakes have caused different degrees of damage to liquid storage structures (LSSs). Due to the particularity of these types of structures, their failure can cause several problems, such as liquid leakage, fire and environment pollution. Base isolation has been widely used as an effective way to improve the seismic capacity of these kinds of structures.

Currently, studies on the energy dissipation of LSSs are more concentrated on rubber isolation [1–5], and some researches show that rubber isolation can reduce the dynamic responses of the structure, but it has very limited reduction effect on wave height or even has opposite effect [6–8]. In addition to rubber isolation, scholars have also explored other energy dissipation methods for LSSs [9–15], and some researches show that friction sliding isolation could be better than that of ordinary rubber isolation [16,17], so it is valuable to study the application of sliding isolation in concrete RLSS.

✉ Xuansheng Cheng
chengxuansheng@gmail.com

1 Key Laboratory of Disaster Prevention and Mitigation in Civil Engineering of Gansu Province, Lanzhou University of Technology, Lanzhou 730050, People's Republic of China

2 Western Engineering Research Center of Disaster Mitigation in Civil Engineering of Ministry of Education, Lanzhou University of Technology, Lanzhou 730050, People's Republic of China

3 Gansu Huaheng Construction and Installation Co., Ltd, Lanzhou 730050, People's Republic of China

The effect of bidirectional earthquake on the structure can't be ignored, but researches on sliding isolation structure under bidirectional earthquake are limited. Jangid [18] studied the responses of sliding isolation structures under two component horizontal harmonic and real ground motion and found that the bidirectional interaction effects were more significant for low- frequency excitation. Zhu and Lv [19] found that the axial force of sliding friction bearing was larger under the action of horizontal bidirectional earthquakes by experimental study, and the change of axial force would affect the friction force and isolation effect. Shrimali and Jangid [13] considered the interaction of frictional forces in two horizontal directions, conducted a parametric study to investigate the effects of important system parameters on the effectiveness of seismic isolation of the liquid storage tanks, and found that the bidirectional interaction of frictional forces had noticeable effects, but the dependence of the friction coefficient on relative velocity of the sliding bearings had no significant effects on the peak response of the isolated liquid storage tanks. Fan et al. [20] studied the sliding displacement of a sliding structure subjected to bidirectional earthquake and found that the sliding displacement may be underestimated and the acceleration of the superstructure may be overrated if the bidirectional interaction of frictional forces is neglected. Based on the comparison of the dynamic responses of friction pendulum sliding isolation structure under unidirectional and bidirectional seismic actions, Wang et al. [21] found that the bidirectional horizontal ground motion had a great influence on structural displacement and acceleration.

In summary, if the design is reasonable, sliding isolation can have good damping effects on the dynamic responses of LSS and wave height at the same time. Besides, bidirectional seismic action has a significant effect on base-isolated structure. In this paper, in order to explore how to reduce the dynamic responses of concrete RLSS and wave height at the same time, friction sliding isolation with displacement-limiting devices for damping method is proposed based on existing energy dissipation methods for LSSs. The simplified mechanical model and dynamic equation of the system are established, and numerical calculation model is established by finite element analysis software ADINA (Automatic Dynamic Incremental Nonlinear Analysis). The effects of friction sliding isolation with displacement-limiting devices on the dynamic responses of concrete RLSS are studied, the dynamic responses under unidirectional and bidirectional earthquake actions are compared, and parameters analysis is also conducted. Finally, intuitive seismic decrease coefficient is used to evaluate the reduction effect of sliding isolation on concrete RLSS.

2 Hybrid Control System with Sliding Isolation and Displacement-Limiting Devices

In studies of the energy dissipation of an LSS, it is better to reduce the structural dynamic responses and wave height simultaneously. For an LSS without a cover plate, when the wave height is too high, liquid leakage will occur. For an LSS with a cover plate, excessively large wave height will cause cover plate destruction because of the liquid impact force [22]. Moreover, the demand for no-water wall will increase with increase in wave height, and the construction cost will also increase. Therefore, to improve the seismic capacities of LSSs and save costs, it is necessary to study new seismic reduction methods.

The damping system proposed in this paper (Fig. 1) can use sand, waste glass and new materials to form a sliding surface at the bottom of RLSSs assuming the periods of tank and isolation system are well separated and isolation surface is properly designed. Then, the base-isolated RLSS will move approximately like a rigid body under the action of some large earthquakes, and its dynamic responses can be controlled effectively. To avoid damage to accessory pipelines because of large deformation differences, the arc displacement-limiting devices are arranged at the bottom of RLSS. Reasonably designed limiting devices can achieve displacement limitation, energy dissipation. For steel limiting devices, when the deformation is in elastic state, they can have the function of self-centering to a certain degree; for more important RLSSs, in order to improve their self-centering capability, more expensive limiting devices made of shape memory alloy (SMA) can be used.

2.1 Simplified Model and Dynamic Equation

Currently, the spring–mass model is often used for the simplified models of LSSs, and it can generally evaluate the dynamic responses accurately [23]. The whole liquid is simplified by the two-particle mass–spring model and divided into two parts [24,25], namely mass m_0, which is attached rigidly to the structure and moves with the structure, and convective mass m_c, which cause sloshing effect. In addition, the mass of concrete structure is large; thus, in dynamic analysis, the concrete mass should be considered. Due to the assumption that the liquid mass m_0 moves with the concrete RLSS, to simplify the model and reduce the degrees of freedom, the concrete structure mass m and liquid mass m_0 can be summed. Sliding material is installed at the structure bottom, which quality with respect to the structure and liquid is negligible. As a result, the structure and the liquid above the isolation layer are used for mass term. A simplified mechanical model of concrete RLSS with sliding base isolation and displacement-limiting devices under bidirectional earthquake actions is shown in Fig. 2.

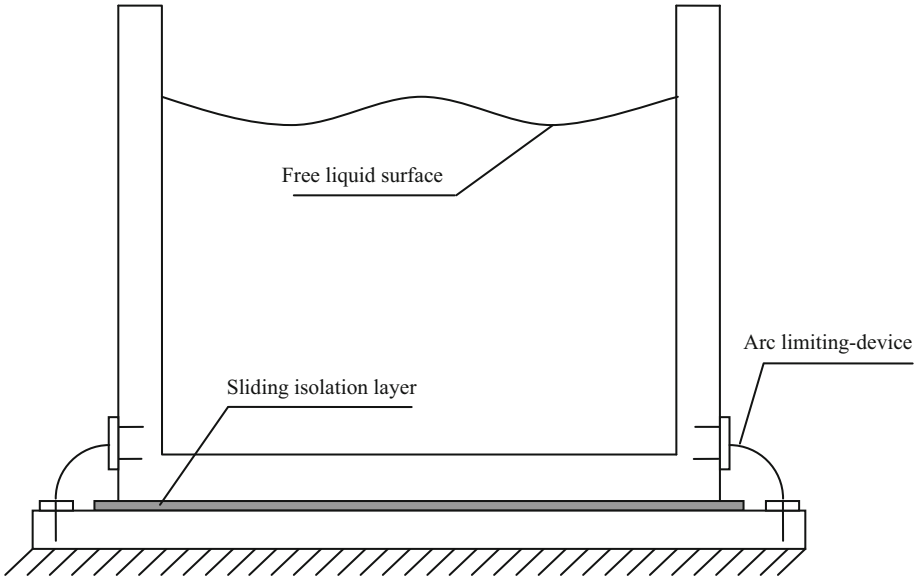

Fig. 1 Schematic diagram of hybrid control system

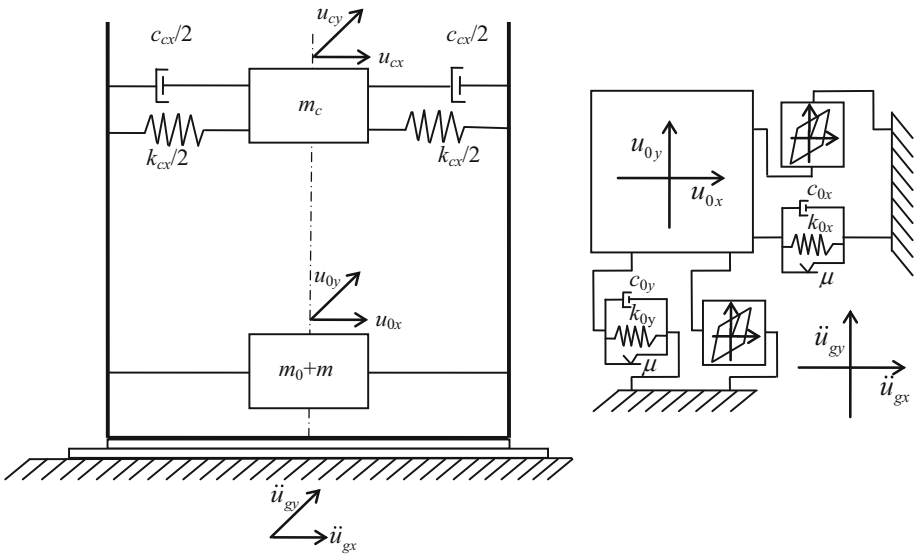

Fig. 2 Simplified model of sliding isolation concrete RLSS with limiting devices

Dynamic equation of the system can be obtained by the Hamilton principle:

$$\mathbf{M}\ddot{\mathbf{U}} + \mathbf{C}\dot{\mathbf{U}} + \mathbf{K}\mathbf{U} = \mathbf{F}_{\mathrm{e}} - \mathbf{F}_{\mathrm{f}} - \mathbf{F}_{\mathrm{s}} \tag{1}$$

$$\mathbf{M} = \begin{bmatrix} m_{cx} & & & \\ & m + m_{0x} & & \\ & & m_{cx} & \\ & & & m + m_{0x} \end{bmatrix};$$

$$\ddot{\mathbf{U}} = \begin{Bmatrix} \ddot{u}_{cx} \\ \ddot{u}_{0x} \\ \ddot{u}_{cy} \\ \ddot{u}_{0y} \end{Bmatrix};$$

$$\mathbf{C} = \begin{bmatrix} c_{cx} & -c_{cx} & & \\ -c_{cx} & c_{0x} + c_{cx} & & \\ & & c_{cy} & -c_{cy} \\ & & -c_{cy} & c_{0y} + c_{cy} \end{bmatrix};$$

$$\dot{\mathbf{U}} = \begin{Bmatrix} \dot{u}_{cx} \\ \dot{u}_{0x} \\ \dot{u}_{cy} \\ \dot{u}_{0y} \end{Bmatrix};$$

$$\mathbf{K} = \begin{bmatrix} k_{cx} & -k_{cx} & & \\ -k_{cx} & k_{0x} + k_{cx} & & \\ & & k_{cy} & -k_{cy} \\ & & -k_{cy} & k_{0y} + k_{cy} \end{bmatrix};$$

$$\mathbf{U} = \begin{Bmatrix} u_{cx} \\ u_{0x} \\ u_{cy} \\ u_{0y} \end{Bmatrix}; \quad \mathbf{F}_{\mathrm{e}} = -\begin{bmatrix} m_{\mathrm{c}}\ddot{u}_{gx} \\ (m + m_0)\,\ddot{u}_{gx} \\ m_{\mathrm{c}}\ddot{u}_{gy} \\ (m + m_0)\,\ddot{u}_{gy} \end{bmatrix};$$

$$\mathbf{F}_{\mathrm{f}} = \begin{Bmatrix} 0 \\ F_{fx} \\ 0 \\ F_{fy} \end{Bmatrix} = \mu M g \begin{Bmatrix} 0 \\ \mathrm{sgn}\,(\dot{u}_{0x}) \\ 0 \\ \mathrm{sgn}\,(\dot{u}_{0y}) \end{Bmatrix};$$

$$\mathbf{F}_{\mathrm{s}}=\left\{\begin{array}{c}0\\ f_{\mathrm{s}}\left(u_{0x}\right)\\ 0\\ f_{\mathrm{s}}\left(u_{0y}\right)\end{array}\right\}$$

where $\mathbf{M}$, $\mathbf{C}$ and $\mathbf{K}$ are mass, damping and stiffness matrices; $\ddot{\mathbf{U}}$, $\dot{\mathbf{U}}$ and $\mathbf{U}$ are acceleration, velocity and displacement vectors; $\mathbf{F}_{\mathrm{e}}$ is seismic force vector; $\mathbf{F}_{\mathrm{f}}$ is friction force vector; $\mathbf{F}_{\mathrm{s}}$ is restoring force vector provided by limiting devices; m_0+m, k_0 and c_0 are the mass, stiffness and damping corresponding to the combination of structure mass m and liquid mass m_0, respectively; u_{c}, $\dot{u}_{\mathrm{c}}$ and $\ddot{u}_{\mathrm{c}}$ are the displacement, velocity and acceleration corresponding to the liquid convection mass m_{c}, respectively; u_0, $\dot{u}_0$ and $\ddot{u}_0$ are the displacement, velocity and acceleration corresponding to the combination of structure mass m and liquid mass m_0, respectively; and $\ddot{u}_{\mathrm{g}}$ is earthquake acceleration. $\mathrm{sgn}(\dot{u}_0)$ is a sign function; when $\dot{u}_0$ is greater than zero, its value is 1; when $\dot{u}_0$ is less than zero, its value is -1; and when $\dot{u}_0$ equals 0, its value is zero. M is the total mass of the system, $M=m_{\mathrm{c}}+m_0+m$; μ is the friction coefficient of sliding isolator, which provide damping effect for the sliding isolation layer; g is the gravitational acceleration; and f_{s} is the restoring force provided by displacement-limiting devices, and the subscripts x and y represent horizontal x-axis and y-axis directions.

The parameters of Eq. (1) can be obtained by Eqs. (2)–(7) [25]:

$$m_{cx}=0.264\frac{L}{h_{\mathrm{w}}}\tanh\left(3.16\frac{h_{\mathrm{w}}}{L}\right)M_{\mathrm{L}} \tag{2}$$

$$m_{0x}=\frac{\tanh\left(0.866\frac{L}{h_{\mathrm{w}}}\right)}{0.866\frac{L}{h_{\mathrm{w}}}}M_{\mathrm{L}} \tag{3}$$

$$h_{cx}=\left[1-\frac{\cosh\left(3.16\frac{h_{\mathrm{w}}}{L}-1\right)}{3.16\frac{h_{\mathrm{w}}}{L}\sinh\left(3.16\frac{h_{\mathrm{w}}}{L}\right)}\right]h_{\mathrm{w}} \tag{4}$$

$$\begin{cases}h_{0x}=\left(0.5-0.09375\frac{L}{h_{\mathrm{w}}}\right); & \frac{L}{h_{\mathrm{w}}}<1.333\\ h_{0x}=0.375; & \frac{L}{h_{\mathrm{w}}}\geq 1.333\end{cases} \tag{5}$$

$$\omega_{cx}=\sqrt{\frac{g\pi}{L}\tanh\left(\frac{\pi h_{\mathrm{w}}}{L}\right)};\ k_{\mathrm{cx}}=\omega_{\mathrm{c}}^2 m_{\mathrm{c}};$$
$$c_{cx}=2\xi_{\mathrm{c}}\sqrt{k_{\mathrm{c}}m_{\mathrm{c}}} \tag{6}$$

$$k_{0x}=\left(\frac{2\pi}{T_x}\right)^2\left(m_{0x}+m\right);$$
$$c_{0x}=2\left(\frac{2\pi}{T_x}\right)\xi_0\left(m_{0x}+m\right) \tag{7}$$

where M_{L} is the total liquid mass and $m_{\mathrm{c}}+m_0$ is equal to M_{L}; h_{w} is liquid height; L is the length of the liquid storage structure, which is parallel to the earthquake direction; h_{c} is the distance between the liquid convective mass and the structure bottom, and h_0 is the distance between the rigid mass and the structure bottom; ω_{c} is circular frequencies corresponding to the convection mass; T_x is isolation period; ξ_{c} is liquid sloshing damping ratio, and it is equal to 0.005; and ξ_0 is the mass damping ratio corresponding to m_0+m, and it is equal to 0.05.

The simplified model parameters in y-axis direction can be obtained by replacing structure length L in Eqs. (2)–(6) with structure width B; at the same time, T_x in Eq. (7) should be replaced with T_y.

2.2 Numerical Calculation Method and Dynamic Equation

Based on the theory of liquid sloshing, the fluid motion equations can be obtained by the fluid dynamics theory:

$$\mathbf{Hp}+\mathbf{A}\dot{\mathbf{p}}+\mathbf{E}\ddot{\mathbf{p}}+\rho_{\mathrm{f}}\mathbf{B}\ddot{\mathbf{r}}+\mathbf{q}_0=0 \tag{8}$$

The structural motion equation in contact with the fluid is:

$$\mathbf{M}_{\mathrm{s}}\ddot{\mathbf{r}}+\mathbf{C}_{\mathrm{s}}\dot{\mathbf{r}}+\mathbf{K}_{\mathrm{s}}\mathbf{r}-\mathbf{B}^{\mathrm{T}}\mathbf{p}=-\mathbf{M}_{\mathrm{s}}\ddot{\mathbf{u}}_{\mathrm{g}}-\mathbf{F}_{\mathrm{f}}-\mathbf{F}_{\mathrm{s}} \tag{9}$$

FSI is achieved by pressure vector $\mathbf{p}$ and coefficient matrix $\mathbf{B}$ in Eqs. (8) and (9), and the coupling motion equation of the system can be obtained by the combination of Eqs. (8) and (9):

$$\begin{bmatrix}\mathbf{M}_{\mathrm{s}} & 0\\ \rho_{\mathrm{f}}\mathbf{B} & E\end{bmatrix}\begin{bmatrix}\ddot{\mathbf{r}}\\ \ddot{\mathbf{p}}\end{bmatrix}+\begin{bmatrix}\mathbf{C}_{\mathrm{s}} & 0\\ 0 & \mathbf{A}\end{bmatrix}\begin{bmatrix}\dot{\mathbf{r}}\\ \dot{\mathbf{p}}\end{bmatrix}+\begin{bmatrix}\mathbf{K}_{\mathrm{s}} & -\mathbf{B}^{\mathrm{T}}\\ 0 & \mathbf{H}\end{bmatrix}\begin{bmatrix}\mathbf{r}\\ \mathbf{p}\end{bmatrix}=\begin{bmatrix}-\mathbf{M}_{\mathrm{s}}\ddot{\mathbf{u}}_{\mathrm{g}}-\mathbf{F}_{\mathrm{f}}-\mathbf{F}_{\mathrm{s}}\\ -\mathbf{q}_0\end{bmatrix} \tag{10}$$

where $\mathbf{M}_{\mathrm{s}}$, $\mathbf{C}_{\mathrm{s}}$ and $\mathbf{K}_{\mathrm{s}}$ are mass, damping and stiffness matrices; $\mathbf{r}$ is displacement vector; $\ddot{\mathbf{u}}_{\mathrm{g}}$ is earthquake acceleration vector; $\mathbf{F}_{\mathrm{f}}$ is friction force vector; $\mathbf{F}_{\mathrm{s}}$ is restoring force vector provided by limiting devices; ρ_{f} is liquid density; $\mathbf{p}$ is liquid pressure vector; $\mathbf{q}_0$ is input excitation vector acting on liquid from structure; $\mathbf{H}$, $\mathbf{A}$, $\mathbf{E}$ and $\mathbf{B}$ are coefficient matrices, and their detail expressions are shown in Eq. (11); and N is shape function.

$$\begin{cases}\mathbf{H}=\iiint_{\Omega}\nabla N\nabla N\mathrm{d}\Omega\\ \mathbf{A}=\frac{1}{C}\iint_{S_{\mathrm{r}}}NN^{\mathrm{T}}\mathrm{d}S_{\mathrm{r}}\\ \mathbf{E}=\frac{1}{C^2}\iiint_{\Omega}NN^{\mathrm{T}}\mathrm{d}\Omega+\frac{1}{g}\iint_{S_{\mathrm{F}}}NN^{\mathrm{T}}\mathrm{d}S_{\mathrm{F}}\\ \mathbf{B}=\left(\iint_{S_{\mathrm{l}}}NN_{\mathrm{S}}^{\mathrm{T}}\mathrm{d}S_{\mathrm{l}}\right)A\end{cases} \tag{11}$$

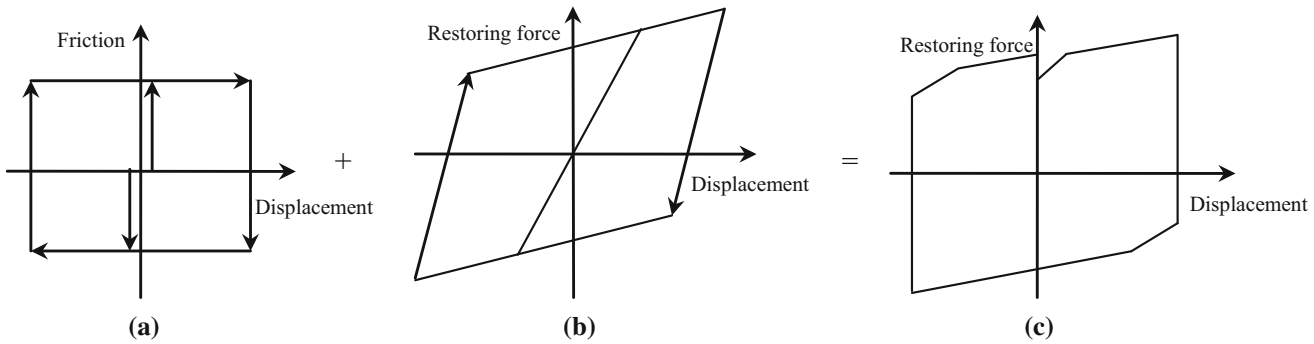

Fig. 3 Restoring force model. **a** Rigid plastic restoring force model. **b** Bilinear restoring force model. **c** Comprehensive restoring force model

Table 1 Material parameters of displacement-limit device

Elastic modulus E/Pa	Poisson's ratio ν	Yield strength σ/MPa	Density ρ/kg/m^3	Strain hardening modulus E/Pa	Yield strain ε	Maximum plastic strain ε_u
2×10^{11}	0.3	235	7800	2×10^9	0.001	0.02

Table 2 Properties of the isolation layer

Properties	μ	Tensile strength	Compressive strength	Usage temperature	Linear expansion coefficient
Values	0.04–0.15	10–25 MPa	12 MPa	−250 to 260 °C	$8^{-25} \times 10^{-5}$/°C

2.3 Restoring Force Model

For the hybrid control system with sliding isolation and displacement-limiting devices, the friction effect of sliding isolation layer can use the rigid plastic restoring force model [26,27], as shown in Fig. 3a. The bilinear restoring force model is used for displacement-limiting devices, as shown in Fig. 3b. By superposing parallel, the comprehensive restoring force model of the isolation layer can be obtained, as shown in Fig. 3c.

3 Numerical Example

3.1 Calculation Model

Using a chemical plant in Lanzhou, Gansu Province, PRC, as the engineering case study, the size of concrete RLSS is 6 m × 6 m × 4.8 m, and its wall thickness is 300 mm. Sliding base isolation is used and contact surface is set to simulate the behavior the sliding isolation layer; eight displacement-limiting devices are set up in the four corners of concrete RLSS. Linear elastic material is used for concrete, its elastic modulus is 3×10^{10}Pa, Poisson's ratio is 0.20, density is 2500kg/m^3, and 3D solid element is used for the concrete structure. Bilinear material model and beam element are used for the limiting devices, and the material parameters are shown in Table 1. Potential-based fluid material and 3D fluid element are used to simulate the liquid, its density is 1000 kg/m^3, and the bulk modulus is 2.3×10^9Pa. Teflon sliding isolation layer is used, the friction coefficient of sliding device made of Teflon is small, with the change of the sliding velocity and the pressure of the surface, the change of the friction coefficient is not very big, and the difference between static friction coefficient and sliding friction coefficient is very small; when the compressive stress of the friction surface is greater than a certain value, the Teflon will enter into plastic-flow state under the combined action of the horizontal force and the upper pressure [28]. Therefore, Teflon is an ideal seismic isolation material, and its material properties are shown in Table 2.

El-Centro wave (component of NS direction) is used to conduct the time history analysis, which was recorded from Imperial Valley earthquake in El-Centro station happened on May 18, 1940. It is a typical near-field seismic record. In order to improve computational efficiency, the records of the first 10 s are only chosen, and the acceleration time history curve is shown in Fig. 4. The calculation model of sliding isolation concrete RLSS with displacement-limiting devices considering FSI is established by ADINA, as shown in Fig. 5.

3.2 Dynamic Responses Under Bidirectional Earthquake Action

In order to study the dynamic responses of sliding isolation concrete RLSS with limiting devices subjected to bidirec-

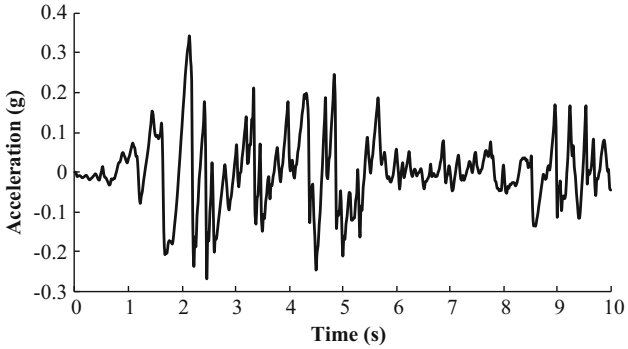

Fig. 4 Acceleration time history curve of El-Centro wave

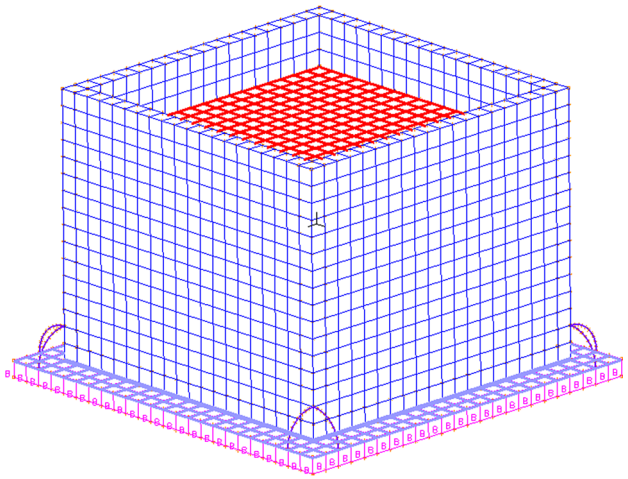

Fig. 5 Numerical calculation model

tional earthquake, the dynamic responses of three types of structures (fixed support structure, pure sliding isolation structure, sliding isolation structure with limiting devices) are compared. The ratio of PGAs in horizontal x-axis and y-axis is adjusted to 1:0.85. Due to limited space, assuming that friction coefficient is 0.06, limiting-device diameter is 60 mm, liquid height is 3.6 m, PGA-x is 0.40 g, and PGA-y is 0.34 g. The calculation results of wave height and structural displacement under bidirectional seismic action are shown in Figs. 6 and 7.

As shown in Fig. 6, under horizontal bidirectional seismic action, wave height of pure sliding isolation and sliding isolation with limiting-devices concrete RLSSs are obviously less than that of fixed support concrete RLSS, and wave height is increased to a certain extent after the limiting devices being taken. As shown in Fig. 7, displacement of pure sliding isolation concrete RLSS is obviously larger than that of sliding isolation with limiting-devices concrete RLSS; namely, for pure sliding isolation concrete RLSS, pounding between sliding isolation structure and surrounding wall will be caused or auxiliary pipelines will be destroyed because of large displacement. After displacement-limiting measure being taken, the horizontal displacement is controlled effectively under horizontal bidirectional seismic action, and the effectiveness of sliding isolation concrete RLSS is improved.

3.3 Comparisons of Dynamic Responses Under Unidirectional and Bidirectional Seismic Actions

In order to investigate the influence of horizontal bidirectional seismic action on the dynamic responses of concrete RLSS, a comparative study on the dynamic responses under unidirectional and bidirectional seismic actions is conducted. The details are shown in Figs. 8, 9 and Table 3.

As shown in Fig. 8, under unidirectional seismic action, the maximum wave heights of fixed support, pure sliding and sliding–limiting concrete RLSS are 0.673, 0.488 and 0.542 m; under bidirectional seismic action, the maximum wave heights of fixed support, pure sliding and sliding–limiting concrete RLSS are 1.24, 0.777 and 1.06 m. As shown in Fig. 9, under unidirectional seismic action, the maximum displacements of pure sliding and sliding–limiting concrete RLSS are 70 and 41.4 mm; under bidirectional seismic action, the maximum displacements of pure sliding and sliding–limiting concrete RLSS are 94.1 and 55.8 m. It is obtained that wave height and structural displacement under bidirectional seismic action are obviously larger than that of unidirectional seismic action, in order to ensure the safety

Fig. 6 Wave height

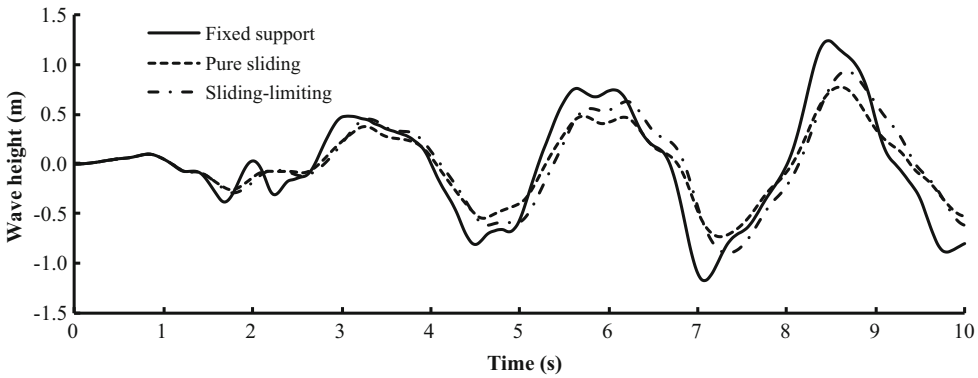

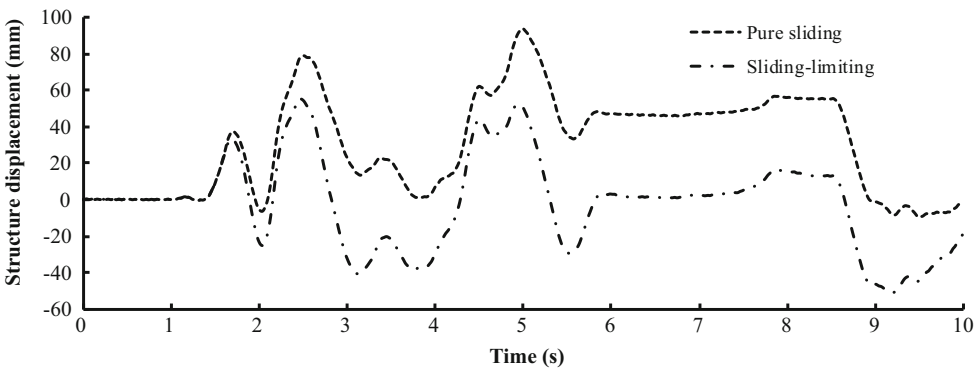

Fig. 7 Structural displacement

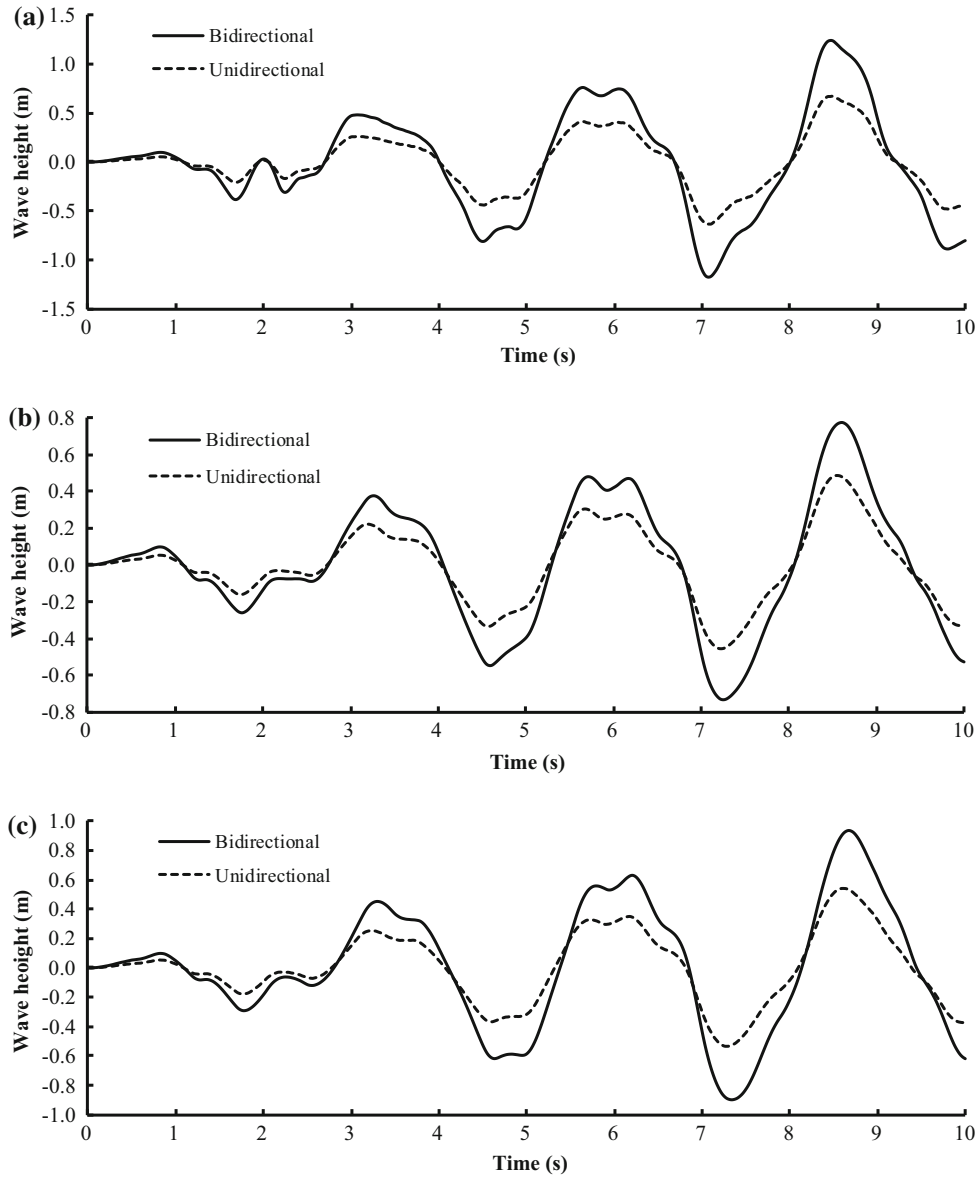

Fig. 8 Influence of bidirectional earthquake on wave height. **a** Fixed support. **b** Pure sliding. **c** Sliding–limiting

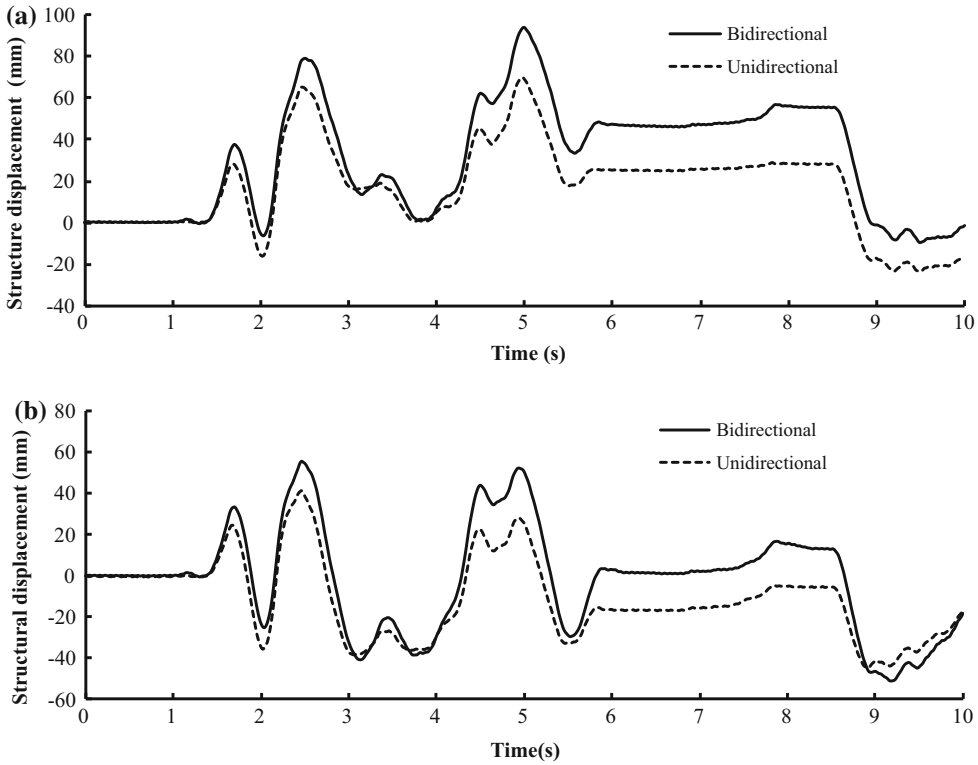

Fig. 9 Influence of bidirectional earthquake on structural displacement. **a** Pure sliding. **b** Sliding–limiting

Table 3 Comparisons of tensile stresses under bidirectional earthquake (MPa)

Action direction	Unidirectional	Bidirectional
Fixed support	1.852	2.702
Pure sliding	1.280	1.443
Sliding–limiting	1.310	1.438

of concrete RLSS under seismic action, it is necessary to consider the influence of bidirectional seismic action in a reasonable way.

As shown in Table 3, compared with unidirectional seismic action, the wall tensile stresses of fixed support, pure sliding and sliding–limiting concrete RLSS under bidirectional seismic action are amplified by 45.90, 12.73 and 9.77%, respectively; namely, horizontal bidirectional seismic action will cause the significant increase in wall tensile stress of concrete RLSS. Besides, the effect of bidirectional earthquake on the wall tensile stress is reduced after sliding isolation being taken. When PGA is 0.40 g, wall tensile stress of fixed support structure is near to concrete tensile strength under unidirectional seismic action, but under bidirectional seismic action, wall tensile stress of fixed support structure has seriously exceeded the tensile strength of concrete, and the wall will be undoubtedly cracked. After sliding isolation is taken for the concrete RLSS, wall tensile stress is effectively controlled whether under unidirectional or bidi-

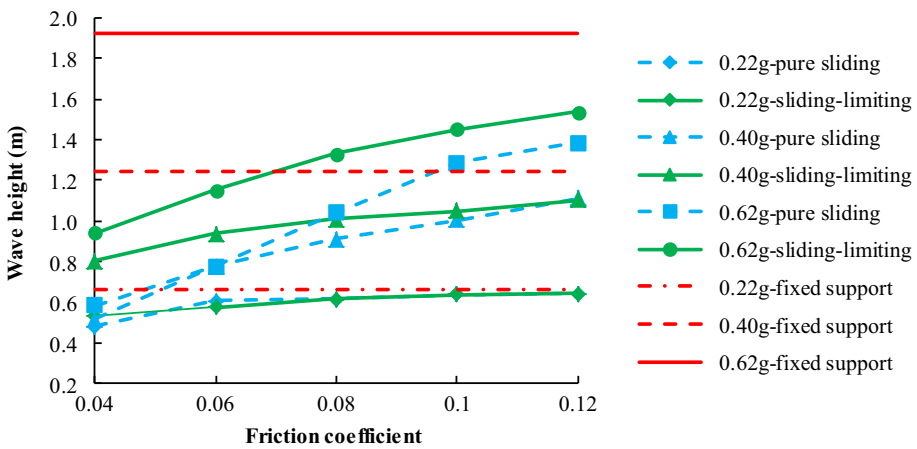

Fig. 10 Influence of friction coefficient on wave height

rectional seismic action, and wall tensile stress is reduced more significantly under bidirectional seismic action.

3.4 Parameter Analysis

3.4.1 Friction Coefficient

Friction coefficient is a very important design parameter of sliding isolation structure, which directly affects the base displacement and damping effect [29]. Liquid level height is 3.6 m, limiting-device diameter is 60 mm, and the influences of friction coefficient on the dynamic responses of the system are shown in Figs. 10, 11 and Table 4.

Figure 10 shows that wave height increases with increase in earthquake intensity and friction coefficient, and the maximum sloshing heights of pure sliding and sliding–limiting structures are less than that of the fixed support structure; namely, sliding base isolation can effectively reduce the wave height. When limiting devices are added to the pure sliding base-isolated structure, the sloshing height slightly increases. The smaller the friction coefficient, the more obvious the reduction effect on the sloshing height. When the friction coefficient is larger and further increases, the differences of wave heights corresponding to isolation structures with and without limiting devices will decrease. Compared with the fixed support structure, the reduction effects of pure sliding and sliding–limiting on the wave height decrease with increase in friction coefficient. When the friction coefficient is large, the advantage of the sliding base-isolated structure cannot be fully employed; therefore, the friction coefficient of sliding base-isolated concrete RLSSs cannot be too large.

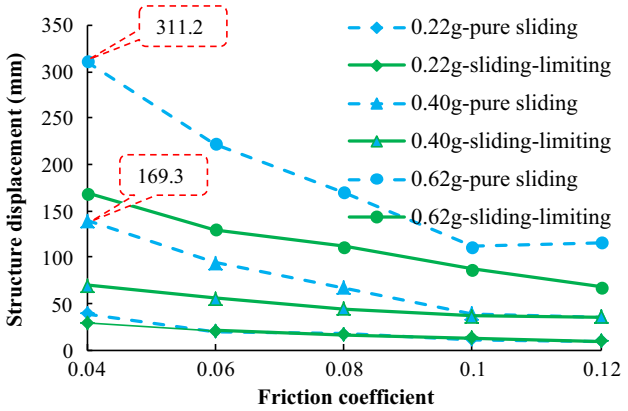

Fig. 11 Influence of friction coefficient on structural displacement

As shown in Fig. 11, the maximum structural displacement increases with increase in earthquake intensity and decreases with increase in friction coefficient. In general, the maximum structural displacement of the pure sliding isolation structure is greater than that of the structure with sliding isolation and displacement-limiting devices. When the friction coefficient is larger, the maximum structural displacement difference between the two types of damping structures is very small. When the earthquake PGAs are 0.22 and 0.40 g, the maximum structural displacement can meet the requirement of the limit value, and the structural displacement difference between the two damping structures is small. However, when the PGA is 0.62 g, the maximum structural displacements of the pure sliding base isolation structures are 311.2 mm, which may exceed the limit of structural displacement. However, after the limiting devices are installed, the maximum structural displacement is reduced to 169.3 mm. Thus, the limiting devices can considerably reduce the structural displacement of pure sliding base-isolated structure and make the structural displacement meet the requirements of the limit value.

As shown in Table 4, for fixed support (no-isolation) structure, when the PGA is 0.22 g, Stress-XX and Stress-YY are 1.786 and 1.760 MPa, which have been close to tensile strength of concrete; however, when the PGA is 0.40 and 0.62 g, the maximum tensile stress of the fixed support structure has exceeds the tensile strength of concrete and will cause the wall to crack (using tensile strength of the concrete as the criterion for concrete crack, and the tensile

Table 4 Effects of friction coefficient on tensile stress

Structure type	Tensile stress		Stress-XX (MPa)					Stress-YY (MPa)				
	Friction coefficient (g)		0.04	0.06	0.08	0.10	0.12	0.04	0.06	0.08	0.10	0.12
Pure sliding	PGA	0.22	1.380	1.451	1.369	1.463	1.431	1.375	1.450	1.365	1.460	1.425
		0.40	1.344	1.445	1.537	1.460	1.683	1.351	1.443	1.529	1.449	1.671
		0.62	1.290	1.312	1.624	1.507	1.653	1.290	1.312	1.624	1.507	1.653
Sliding–limiting	PGA	0.22	1.281	1.264	1.407	1.463	1.419	1.280	1.264	1.407	1.463	1.415
		0.40	1.326	1.431	1.519	1.420	1.854	1.297	1.438	1.516	1.429	1.848
		0.62	1.527	1.322	1.664	1.672	1.678	1.513	1.327	1.661	1.660	1.662
Fixed support	PGA	0.22	1.786					1.760				
		0.40	2.749					2.702				
		0.62	3.892					3.818				

strength of the concrete used in this engineering is 2.01 MPa). After energy dissipation method being taken, the maximum tensile stresses corresponding to pure sliding structure and sliding–limiting structure are less than that of the fixed support structure, and the tensile stress are all much less than the tensile strength of the concrete (2.01 MPa). Generally, when the friction coefficient is smaller and the earthquake intensity is greater, the reduction effect of sliding base isolation on tensile stress of concrete RLSS is more obvious.

From above analysis, sliding isolation system with low friction coefficient will reduce demand on concrete RLSS more significantly, although structural displacement could be large. In order to better play the advantages of sliding isolation RLSS, low friction coefficient should be chosen, and flexible piping connection and limiting devices can be used to mitigate the adverse effect caused by large displacement of sliding isolation concrete RLSS.

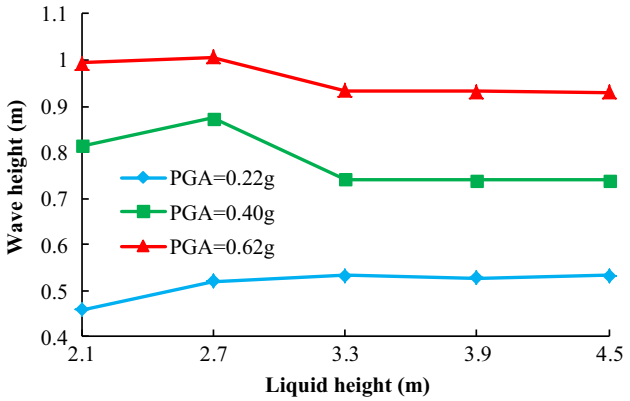

Fig. 12 Effect of liquid height on wave height

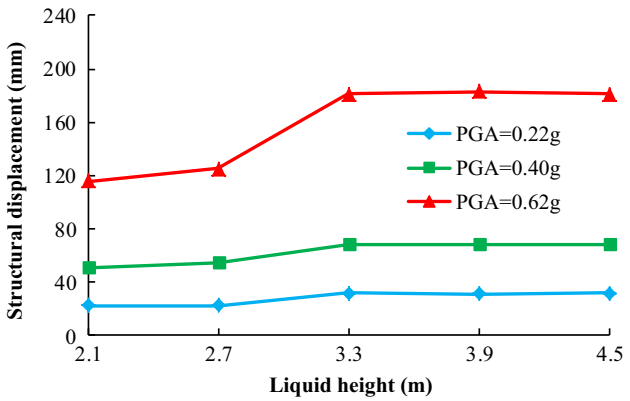

Fig. 13 Effect of liquid height on structural displacement

3.4.2 Liquid Height

The liquid level height of LSS is changeable at different stages due to the requirement of its function; namely, liquid level height is a random variable. In order to investigate the influence of liquid level height on the dynamic responses of the system, assuming that friction coefficient is 0.06, limit-device diameter is 60 mm, the liquid level height is 2.1, 2.7, 3.3, 3.9 and 4.5 m, respectively, and the detailed results are shown in Figs. 12, 13 and Table 5.

As shown in Fig. 12, the influence of liquid level height on wave height is small after damping measures being taken. As shown in Fig. 13, structural displacement increases with the increase of liquid level height, and then, it remains constant; when the PGA is 0.62 g, the influence of liquid level height on structural displacement is greater. As shown in Table 5, the wall tensile stresses under various liquid level heights are much smaller than that of concrete tensile strength; besides, the wall tensile stress increases with the increase in liquid level height on the whole; therefore, in the design of sliding isolation concrete RLSS, it is necessary to take larger liquid filling ratio as the control condition.

3.4.3 Limiting-Device Diameter

The section diameter is an important design parameter of the limiting-device, which directly determines the stiffness of the limiting-device. In order to investigate the influence of limiting-device diameter on the dynamic responses of the system, assuming that limiting-device diameter is 20, 40, 60, 80 and 100 mm, respectively, friction coefficient is 0.06, and liquid level height is 3.6 m. The detailed results are shown in Figs. 14, 15 and Table 6.

As shown in Fig. 14, wave height increases with the increase of limiting-device diameter, and the greater the seismic intensity, the greater the influence of limiting-device diameter on wave height; when the limiting-device diameter is increased to a certain value, the sliding isolation will lose the damping effect on wave height. As shown in Fig. 15, when the PGA is 0.22 g, the influence of limiting-device diameter on structural displacement is small, but when the PGAs are

Table 5 Effect of liquid height on tensile stress

Tensile stress		Stress-XX (MPa)					Stress-YY (MPa)				
Liquid height		2.1 m	2.7 m	3.3 m	3.9 m	4.5 m	2.1 m	2.7 m	3.3 m	3.9 m	4.5 m
PGA	0.22 g	0.485	0.737	0.924	0.956	1.145	0.476	0.687	0.934	0.955	1.136
	0.40 g	0.524	0.877	0.914	0.930	1.226	0.512	0.827	0.902	0.914	1.223
	0.62 g	0.615	0.696	0.925	1.271	1.228	0.566	0.759	0.917	1.274	1.236

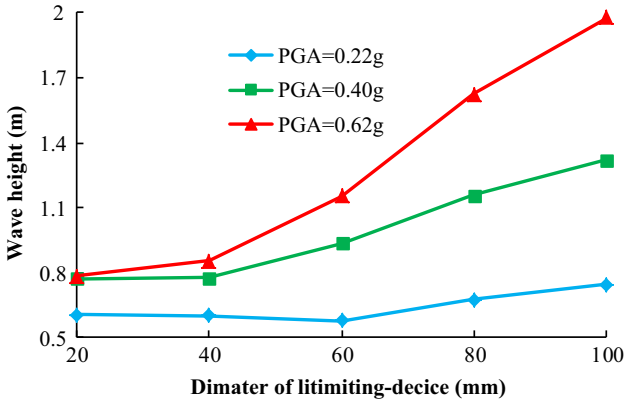

Fig. 14 Effect of limiting-device diameter on wave height

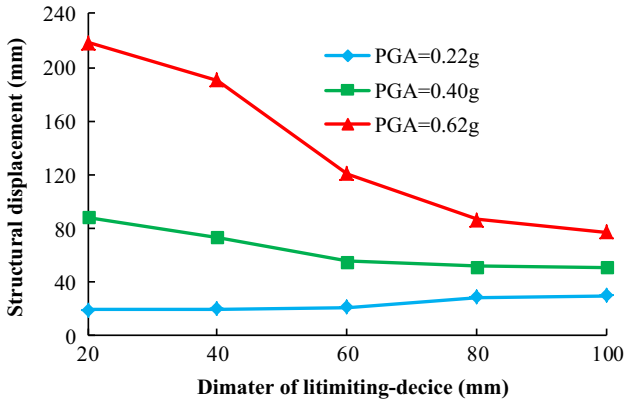

Fig. 15 Effect of limiting-device diameter on structural displacement

0.40 and 0.62 g, the structural displacement decreases with the increase in limiting-device diameter; namely, the greater the earthquake intensity, the greater the influence of limiting-device diameter on structural displacement.

As shown in Table 6, when the limiting-device diameter is increased from 20 to 80 mm, the wall tensile stress is small; however, when the limiting-device diameter is increased to 100 mm, the wall tensile stress is close to or exceeds the tensile strength of concrete. Therefore, the limiting-device diameter is another important factor which affects the damping effect of sliding isolation, and too large limiting-device diameter can make the sliding isolation lose the role of shock absorption. It is suggested that smaller diameter should be used for limiting-device under the premise of structural displacement meeting the requirements.

3.5 Seismic Decrease Coefficient

Seismic decrease coefficient can directly reflect the isolation effect, which can be defined as:

$$R = \frac{Q_{\text{fixed}} - Q_{\text{isolated}}}{Q_{\text{fixed}}} \tag{12}$$

where R is seismic decrease coefficient; Q_{fixed} is dynamic response of no-isolation structure; and Q_{isolated} is dynamic response of isolation structure.

In order to study the seismic decrease coefficient of sliding isolation concrete RLSS with limiting devices, based on the results of parameter analysis, the friction coefficient is assumed as 0.04, limiting-device diameter is 60 mm, and liquid height is 3.6 m. The time history records of different sites of Chi-Chi, Darfield and Loma earthquakes are chosen, and the PGAs in x-axis and y-axis are 0.62 and 0.527 g. Among these records, there are 10 near-field pulse-like earthquake records, 10 near-field no-pulse earthquake records and 10 far-field earthquake records, and their details are shown in Table 7.

The two most common failure modes of concrete liquid storage structures are wall cracking and liquid overflow, based on the calculation of 90 models under the action of horizontal bidirectional earthquakes, the tensile stresses and wave heights corresponding to fixed support, pure sliding and sliding–limiting concrete RLSS are obtained, and the seismic decrease coefficients are calculated by Eq. (12). In order to get the statistical results, the average values of the seismic decrease coefficients are obtained, and the details are shown in Tables 8 and 9.

As shown in Table 8, under horizontal bidirectional near-field pulse-like, near-field no-pulse and far-field earthquake actions, the average seismic decrease coefficients corresponding to tensile stress of pure sliding isolation concrete RLSS are 0.543, 0.581 and 0.568, respectively, and the average seismic decrease coefficients corresponding to tensile stress of sliding isolation concrete RLSS with limiting devices are 0.537, 0.595 and 0.575, respectively.

Table 6 Effect of limiting-device diameter on tensile stress

Tensile stress		Stress-XX (MPa)					Stress-YY (MPa)				
Diameter		20 mm	40 mm	60 mm	80 mm	100 mm	20 mm	40 mm	60 mm	80 mm	100 mm
PGA	0.22 g	1.364	1.349	1.264	1.498	1.959	1.362	1.355	1.262	1.473	1.914
	0.40 g	1.358	1.524	1.431	1.682	2.303	1.357	1.497	1.438	1.676	2.250
	0.62 g	1.318	1.413	1.322	1.509	3.116	1.318	1.426	1.327	1.506	2.937

Table 7 Earthquake information

Near-field pulse-like			Near-field no-pulse			Far-field		
No.	Earthquake	Station	No.	Earthquake	Station	No.	Earthquake	Station
1	Chi-Chi	CHY101	11	Chi-Chi	TCU106	21	Chi-Chi	CHY027
2	Chi-Chi	TCU036	12	Chi-Chi	TCU110	22	Chi-Chi	CHY032
3	Chi-Chi	TCU046	13	Chi-Chi	TCU116	23	Chi-Chi	CHY033
4	Chi-Chi	TCU051	14	Chi-Chi	TCU122	24	Chi-Chi	CHY044
5	Darfield	DSLC	15	Darfield	DFHS	25	Darfield	CSHS
6	Darfield	LINC	16	Darfield	LRSC	26	Darfield	MYAC
7	Darfield	TPLC	17	Darfield	RKAC	27	Darfield	PEEC
8	Loma	Gilory array #3	18	Loma	Capitola	28	Loma	Calaveras Reservoir
9	Loma	Gilory array #2	19	Loma	Gilory array #6	29	Loma	Fremont-Emerson Court
10	Loma	Saratoga-W valley coll	20	Loma	Gilory array #4	30	Loma	SAGO South-Surface

Table 8 Seismic decrease coefficients corresponding to tensile stress

No.	Seismic decrease coefficient		No.	Seismic decrease coefficient		No.	Seismic decrease coefficient	
	Sliding	Sliding–limiting		Sliding	Sliding–limiting		Sliding	Sliding–limiting
1	0.38	0.38	11	0.75	0.72	21	0.36	0.38
2	0.57	0.52	12	0.35	0.44	22	0.49	0.51
3	0.74	0.73	13	0.48	0.52	23	0.63	0.63
4	0.67	0.70	14	0.68	0.68	24	0.45	0.49
5	0.65	0.65	15	0.77	0.77	25	0.76	0.78
6	0.44	0.44	16	0.51	0.51	26	0.59	0.59
7	0.64	0.63	17	0.62	0.61	27	0.65	0.64
8	0.38	0.38	18	0.60	0.64	28	0.65	0.63
9	0.40	0.40	19	0.65	0.65	29	0.63	0.60
10	0.55	0.53	20	0.41	0.40	30	0.46	0.51
Average	0.543	0.537	Average	0.581	0.595	Average	0.568	0.575

Table 9 Seismic decrease coefficients corresponding to wave height

No.	Seismic decrease coefficient		No.	Seismic decrease coefficient		No.	Seismic decrease coefficient	
	Sliding	Sliding–limiting		Sliding	Sliding–limiting		Sliding	Sliding–limiting
1	0.41	0.35	11	0.45	0.41	21	0.44	0.32
2	0.46	0.38	12	0.42	0.36	22	0.46	0.39
3	0.56	0.49	13	0.49	0.38	23	0.40	0.33
4	0.46	0.40	14	0.44	0.37	24	0.49	0.41
5	0.51	0.42	15	0.48	0.39	25	0.55	0.48
6	0.48	0.39	16	0.46	0.35	26	0.46	0.40
7	0.52	0.47	17	0.49	0.40	27	0.51	0.42
8	0.49	0.44	18	0.51	0.42	28	0.48	0.38
9	0.45	0.36	19	0.50	0.40	29	0.46	0.37
10	0.47	0.38	20	0.48	0.39	30	0.52	0.43
Average	0.481	0.408	Average	0.472	0.387	Average	0.477	0.393

As shown in Table 9, under horizontal bidirectional near-field pulse-like, near-field no-pulse and far-field earthquake actions, the average seismic decrease coefficients corresponding to wave height of pure sliding isolation concrete RLSS are 0.481, 0.472 and 0.477, respectively, and the average seismic decrease coefficients corresponding to wave height of sliding isolation concrete RLSS with limiting devices are 0.408, 0.387 and 0.393, respectively.

Through the comparison of the two kinds of seismic decrease coefficients, it is obtained that the influence of limiting-device on the wave height is greater than that of the wall tensile stress. Besides, the seismic decrease coefficients corresponding to wall tensile stress and wave height under different kinds of bidirectional earthquakes are large, so the effectiveness of sliding isolation on concrete RLSS is further verified.

4 Conclusions

In order to improve the safety of concrete RLSS under earthquake action, a energy dissipation method of sliding isolation and limiting devices for concrete RLSS is proposed, the dynamic responses of sliding isolation concrete RLSS under bidirectional earthquake are studied, a parameter analysis is conducted, and finally, the effectiveness and the significance of the energy dissipation method are further verified by the seismic decrease coefficients corresponding to wall tensile stress and wave height. The main conclusions are as follows:

1. Sliding isolation can effectively reduce the wall tensile stress of concrete RLSS, but the larger the friction coefficient, the liquid lever height and the limiting-device diameter are, the wall tensile stress will be also larger on the whole.
2. The maximum wave height of sliding isolation concrete RLSS is less than that of fixed support concrete RLSS, and the smaller the friction coefficient is, the greater the seismic intensity is, the more obvious the reduction effect of sliding isolation on wave height.
3. The structural displacement, wave height and wall tension stress under bidirectional seismic action are significantly higher than those of under unidirectional earthquake action.
4. Setting limiting devices can solve the problem that the displacement of sliding isolation concrete RLSS exceeds the limit under the condition of large earthquake intensity and small friction coefficient, but it should be noted that larger limiting-device diameter may make sliding isolation lose the shock absorption effect. In order to further improve the security of the system, when the friction coefficient is small, besides the limiting devices, the flexible connection should be adopted in the auxiliary pipeline of LSS, so as to deal with the adverse effects caused by the large structure displacement.
5. Based on the analysis of sliding isolation concrete RLSS with limiting devices under near-field pulse-like, near-field no-pulse and far-field earthquakes, it is obtained that the seismic decrease coefficients corresponding to wall tensile stress and wave height are all large enough; therefore, sliding isolation with limiting-devices system is of great significance to the control of the two most common failure modes of concrete RLSS, namely wall cracking and liquid overflow.

Acknowledgements This paper is a part of the National Natural Science Foundation of China (Grant Number: 51368039, 51478212), a part of the Education Ministry Doctoral Tutor Foundation of China (Grant Number: 20136201110003) and a part of the Plan Project of Science and Technology in Gansu Province (Grant Number: 144GKCA032).

References

1. Malhotra, P.K.: New method for seismic isolation of liquid-storage tanks. Earthq. Eng. Struct. Dyn. **26**(8), 839–847 (1997). doi:10.1002/(SICI)1096-9845(199708)26:8
2. Li, Z.L.; Li, Y.; Li, H.B.: Parametric research on seismic response of large scale liquid storage tank isolated by lead-rubber bearings. J. Sichuan Univ. Eng. Sci. Ed. **42**(5), 134–141 (2010)
3. Yang, Z.R.; Shou, B.N.; Sun, L.; Wang, J.J.: Earthquake response analysis of spherical tanks with seismic isolation. Procedia Eng. **14**(11), 1879–1886 (2011). doi:10.1016/j.proeng.2011.07.236
4. Cheng, X.S.; Cao, L.L.; Zhu, H.Y.: Liquid–solid interaction seismic response of an isolated overground rectangular reinforced-concrete liquid-storage structure. J. Asian Archit. Build. Eng. **14**(1), 175–180 (2015). doi:10.3130/jaabe.14.175
5. Cheng, X.S.; Zhao, L.; Zhang, A.J.: FSI resonance response of liquid-storage structures made of rubber-isolated rectangular reinforced concrete. Electron. J. Geotech. Eng. **20**(7), 1809–1824 (2015)
6. Chalhoub, M.S.; Kelly, J.M.: Shake table test of cylindrical water tanks in base-isolated structures. J. Eng. Mech. Am. Soc. Civil Eng. **116**(7), 1451–1472 (1990)
7. Shekari, M.R.; Khaji, N.; Ahmadi, M.T.: A coupled BE–FE study for evaluation of seismically isolated cylindrical liquid storage tanks considering fluid-structure interaction. J. Fluids Struct. **25**(3), 567–585 (2009). doi:10.1016/j.jfluidstructs.2008.07.005
8. Vosoughifar, H.; Naderi, M.: Numerical analysis of the base-isolated rectangular storage tanks under bi-directional seismic excitation. Br. J. Math. Comput. Sci. **4**, 3054–3067 (2014). doi:10.9734/BJMCS/2014/11299
9. Wang, Y.P.; Teng, M.C.; Chung, K.W.: Seismic isolation of rigid cylindrical tanks using friction pendulum bearings. Earthq. Eng. Struct. Dyn. **30**(7), 1083–1099 (2001)
10. Wen, L.; Wang, S.G.; Du, D.S.; Xu, L.P.: Controlling analysis of friction pendulum system for the seismic isolation of liquid storage tanks. World Earthq. Eng. **25**(4), 161–166 (2009)
11. Panchal, V.R.; Jangid, R.S.: Seismic response of liquid storage steel tanks with variable frequency pendulum isolator. KSCE J. Civil Eng. **15**(6), 1041–1055 (2011). doi:10.1007/s12205-011-0945-y
12. Abalı, E.; Uçkan, E.: Parametric analysis of liquid storage tanks base isolated by curved surface sliding bearings. Soil Dyn Earthq. Eng. **30**(1), 21–31 (2010). doi:10.1016/j.soildyn.2009.08.001

13. Shrimali, M.K.; Jangid, R.S.: Seismic response of liquid storage tanks isolated by sliding bearings. Eng. Struct. **24**(7), 909–921 (2002)
14. Zhang, Z.L.; Gao, B.Q.; Yang, H.K.: Seismic analysis of a large base-isolated liquid storage tank with fixed roof based on added mass method. J. Vib. Shock **31**(23), 32–38 (2012). doi:10.13465/j.cnki.jvs.2012.23.015
15. Soni, D.P.; Mistry, B.B.; Panchal, V.R.: Double variable frequency pendulum isolator for seismic isolation of liquid storage tanks. Nucl. Eng. Des. **241**(3), 700–713 (2011). doi:10.1016/j.nucengdes.2011.01.012
16. Zhang, R.F.; Weng, D.G.; Ren, X.S.: Seismic analysis of a LNG storage tank isolated by a multiple friction pendulum system. Earthq. Eng. Eng. Vib. **10**(2), 253–262 (2011). doi:10.1007/s11803-011-0063-3
17. Seleemah, A.A.; El-Sharkawy, M.: Seismic response of base isolated liquid storage ground tanks. Ain Shams Eng. J. **2**(1), 33–42 (2011). doi:10.1016/j.asej.2011.05.001
18. Jangid, R.S.: Response of pure-friction sliding structures to bi-directional harmonic ground motion. Eng. Struct. **19**(2), 97–104 (1997). doi:10.1016/S0141-0296(96)00055-7
19. Zhu, Y.H.; Lv, X.L.: Shaking table tests of model building with sliding isolation system under multi-direction ground motions. Earthq. Eng. Eng. Vib. **22**(5), 77–84 (2002). doi:10.13197/j.eeev.2002.05.015
20. Fan, A.W.; Tang, J.X.; Li, L.; Yang, J.: Study on the sliding displacement of a sliding structure subjected to multi-directional earthquake excitation. J. Earth Sci. **16**(1), 79–83 (2005)
21. Wang, J.Q.; Feng, J.C.; Li, D.W.: Analysis on seismic response of base-isolated structures with friction pendulum system under multi-axial ground motions. World Earthq. Eng. **25**(4), 92–96 (2009)
22. Minowa, C.; Ogawa, N.; Harada, I.: Sloshing roof impact tests of a rectangular tank. Am. Soc. Mech. Eng. Press. Vessel. Pip. Div. (Publ.) **272**, 13–21 (1994)
23. Ge, Q.Z.; Weng, D.G.; Zhang, R.F.: A nonlinear simplified model of liquid storage tank and primary resonance analysis. Eng. Mech. **31**(5), 166–171 (2014). doi:10.6052/j.issn.1000-4750.2012.12.0944
24. Housner, G.W.: The dynamic behavior of water tanks. Bull. Seismol. Soc. Am. **53**(2), 381–387 (1963)
25. ACI Committee 350: Seismic Design of Liquid-containing Concrete Structures (ACI 350.3-01) and Commentary (ACI 350.3R-01). American Concrete Institute. Farmington Hills, MI (2001)
26. Rong, Q.; Sheng, Y.; Cheng, W.R.: Experimental investigation and mechanical model of sliding isolation bearings. Eng. Mech. **27**(12), 40–45 (2010)
27. Wang, C.F.; Chen, X.C.; Zhu, C.L.; Xia, X.S.: The contact-and-friction element considering nonlinear performance of movable supports and restrainers. Eng. Mech. **30**(8), 186–192 (2013)
28. Xiong, Z.M.; Huo, X.P.; Su, N.N.: Theoretical analysis of a new kind of sliding base isolation frame structure. J. Vib. Shock **27**(10), 124–129 (2008). doi:10.13465/j.cnki.jvs.2008.10.033
29. Chakraborty, S.; Roy, K.; Ray-Chaudhuri, S.: Design of re-centering spring for flat sliding base isolation system: theory and a numerical study. Eng. Struct. **126**, 66–77 (2016). doi:10.1016/j.engstruct.2016.07.049